PHYSICAL REVIEW D **96,** 056026 (2017)

Imprints of a light sterile neutrino at DUNE, T2HK, and T2HKK

Sandhya Choubey,[1,2,3,*] Debajyoti Dutta,[1,3,†] and Dipyaman Pramanik[1,3,‡]

[1]*Harish-Chandra Research Institute, Chhatnag Road, Jhunsi, Allahabad 211 019, India*

[2]*Department of Theoretical Physics, School of Engineering Sciences, KTH Royal Institute of Technology, AlbaNova University Center, 106 91 Stockholm, Sweden*

[3]*Homi Bhabha National Institute, Training School Complex, Anushakti Nagar, Mumbai 400085, India*

(Received 2 May 2017; published 28 September 2017)

We evaluate the impact of sterile neutrino oscillations in the so-called $3+1$ scenario on the proposed long baseline experiment in USA and Japan. There are two proposals for the Japan experiment which are called T2HK and T2HKK. We show the impact of sterile neutrino oscillation parameters on the expected sensitivity of T2HK and T2HKK to mass hierarchy, *CP* violation and octant of θ_{23} and compare it against that expected in the case of standard oscillations. We add the expected ten years data from DUNE and present the combined expected sensitivity of T2HKK + DUNE to the oscillation parameters. We do a full marginalization over the relevant parameter space and show the effect of the magnitude of the true sterile mixing angles on the physics reach of these experiments. We show that if one assumes that the source of *CP* violation is the standard *CP* phase alone in the test case, then it appears that the expected *CP* violation sensitivity decreases due to sterile neutrinos. However, if we give up this assumption, then the *CP* sensitivity could go in either direction. The impact on expected octant of θ_{23} and mass hierarchy sensitivity is shown to depend on the magnitude of the sterile mixing angles in a nontrivial way.

DOI: 10.1103/PhysRevD.96.056026

I. INTRODUCTION

The field of neutrino oscillations is on the verge of its final leap forward. The three-generation paradigm has been firmly established and the leading oscillation parameters are determined to very high precision. The last of the neutrino oscillation parameters are expected to be measured with unprecedented precision in the next generation long baseline experiments. In particular, the questions regarding *CP* violation in the lepton sector, the order of the neutrino masses and the octant of the mixing angle θ_{23} are expected to be answered within the next decade. The most promising experiments that the neutrino community is looking forward to in this regard are the Deep Underground Neutrino Experiment (DUNE) in USA [1–4] and the Tokai to Hyper-Kamiokande (T2HK) experiment in Japan [5]. The question on neutrino mass hierarchy should be the first to be resolved with the expected sensitivity reach of DUNE being more than 5σ. The detector for the T2HK experiment in Japan is proposed to be placed at only 295 km and hence with a narrow-band beam peaked at about 0.6 GeV, the expected matter effects in T2HK is low and its mass hierarchy sensitivity rather poor. To circumvent this problem there is a proposal to shift one module and hence half of the HK detector to a location in Korea at a distance of 1100 km. This proposal is referred to as T2HKK (Tokai to Hyper-Kamiokande Korea).[1] This brings a more than 3σ discovery potential for a large fraction of the true *CP* phase $\delta_{13}(\text{true})$. While DUNE is expected to discover *CP* violation at the 3σ level for 75% of the true δ_{13} (with 1320 kt. MW. year) [3], T2HK is expected to discover it at the 5σ level for 55%–60% of the true δ_{13} [6]. The question on the true octant of θ_{23} should be settled at the 5σ level for $\sin^2\theta_{23}(\text{true}) < 0.43$ and $\sin^2\theta_{23}(\text{true}) > 0.59$ with data at DUNE and for $\sin^2\theta_{23}(\text{true}) < 0.46$ and $\sin^2\theta_{23}(\text{true}) > 0.56$ with data at T2HK [5].

Even though neutrino oscillations within the three-generation framework is well established, anomalous hints of neutrino oscillations at a higher frequency corresponding to a mass squared difference $\Delta m^2 \sim 1\ \text{eV}^2$ have been around for a long time [7]. The first such claim came from the LSND experiment [8,9] in Los Alamos, USA, where a $\bar{\nu}_\mu$ beam was sent to a detector and the observations showed a 3.8σ excess in the electrons (positrons) which could be explained in terms of $\bar{\nu}_\mu \to \bar{\nu}_e$ oscillations driven by $\Delta m^2 \sim 1\ \text{eV}^2$. This oscillation claim was tested by the KARMEN [10] and MiniBooNE [11–13] experiments. While KARMEN data did not show any evidence for $\nu_\mu \to \nu_e$ oscillations, it was unable to rule out the entire parameter space allowed by LSND. More recently, the MiniBooNE experiment ran in both the neutrino as well as antineutrino mode. The MiniBooNE collaboration concluded that while they did not see any electron excess in their neutrino event

*sandhya@hri.res.in
†debajyotidutta@hri.res.in
‡dipyamanpramanik@hri.res.in

[1]In this work we will refer to the first module of the megaton HK detector as JD (Japan Detector) while the second module will be called KD (Korea Detector).

 © 2017 American Physical Society

sample consistent with LSND, their antineutrino data shows an excess confirming the oscillations seen by LSND. MiniBooNE reported an excess of electrons/positrons at low energies in both neutrino as well as antineutrino modes, however these excess events are not coming from neutrino flavor oscillations.

More recently, anomalies in the reactor antineutrino flux measurements [14–16] and the gallium experiments calibration data [17–21] have also hinted at the possibility of ν_e (or $\bar{\nu}_e$) oscillations with $\Delta m^2 \sim 1$ eV^2. Since it is not possible to accommodate this extra mass squared difference within the three-generation framework, one needs to add at least one additional light neutrino species and since the Z decay width constrains the number of light neutrinos coupled to the Z-boson to be 2.9840 ± 0.0082 [22], the additional neutrino(s) should not have any standard model gauge interactions. These neutrinos are hence called sterile for this reason. With one additional sterile neutrino, one could have a neutrino mass spectrum of the so-called $2+2$ or $3+1$ type [23], where the former has two lighter neutrinos separated by two heavier ones by $\Delta m^2 \sim 1$ eV^2, while the latter has one heavier state separated by three lighter ones by $\Delta m^2 \sim 1$ eV^2. The $2+2$ mass spectrum predicts oscillations involving the sterile neutrino in either the solar or the atmospheric neutrino sectors. Since neither of the two data sets allows this, the $2+2$ spectrum is heavily disfavored by the solar neutrino and atmospheric neutrino observations, as well as from bounds on the sum of neutrino masses from cosmology [24]. The $3+1$ spectrum on the other hand predicts low admixture of the sterile neutrinos in solar and atmospheric neutrino oscillations and hence survives. It also has only one heavy mass state instead of two and hence has less issues with the bounds from cosmology. Nonetheless, the global analysis of all relevant data sets that constrain the $3+1$ parameter space returns a goodness of fit of only 19% [25]. The main problem with the $3+1$ scenario is the tension between the appearance data in LSND and MiniBooNE and the disappearance data of ν_μ at experiments like CDHS and MINOS.

It has been pointed out [26,27] that the sensitivity of long baseline experiments to standard neutrino oscillation parameters such as neutrino mass hierarchy, CP violation and octant of θ_{23} gets compromised in the presence of sterile neutrino(s). As we will discuss, this happens because even though the oscillations due to the $\Delta m^2 \sim 1$ eV^2 frequency average out at the long baselines, the impact of the additional mixing angles and phases due to the additional sterile neutrinos stay in the relevant oscillation probabilities. The expected sensitivity of the DUNE near detector to the sterile neutrino parameters themselves was studied in [28] while the corresponding sensitivity of the DUNE far detector to these parameters was presented in [29]. The expected sensitivity of T2HK to the sterile neutrino parameters has been studied recently in [30]. The impact of sterile neutrinos on the sensitivity to standard oscillation parameters in T2K and NOνA was discussed in [26,31,32], and in DUNE in [27,29,33–35]. In particular, the expected change to standard neutrino parameter sensitivity of DUNE for the $3+1$ scenario has been given in [29,35], taking into account the marginalization of the sterile neutrino as well as the relevant standard oscillation parameters.

In this work we focus on two main purposes. First, we consider the impact of sterile neutrino mixing in the $3+1$ scenario on the physics reach of the T2HK and T2HKK setups. We calculate the expected sensitivity to neutrino mass hierarchy, CP violation and octant of θ_{23} both in the absence (referred to as the $3+0$ case) as well as presence (referred to as the $3+1$ case) of a sterile neutrino. Second, we present combined analysis of the T2HKK setup with DUNE to check for possible synergies between the two experiments. We present the expected sensitivity of the T2HK and T2HKK setups to the oscillation parameters in both $3+0$ and $3+1$ scenarios.

The paper is organized as follows. We will discuss the oscillation probabilities in the $3+1$ case in Sec. II. The simulation procedure will be given in Sec. III, while the experimental configurations considered in our analyses will be specified in Sec. IV. We will discuss our results and present the expected sensitivities of the T2HK, T2HKK and T2HKK+DUNE configurations in Sec. V. Finally, we will conclude in Sec. VI.

II. STERILE NEUTRINO HYPOTHESIS

In order to explain the short baseline anomalies [7], one or more extra neutrino states of mass squared difference $\sim$1 eV^2 are proposed. But the LEP data suggests that these extra neutrinos must be singlet under the standard model gauge group. Thus they are called sterile neutrinos. For the $3+1$ case, the full neutrino mixing matrix will have six mixing angles, three phases and three mass-squared differences. This mixing matrix can be parametrized in the following way:

$$U^{3+1}_{\rm PMNS} = O(\theta_{34},\delta_{34})O(\theta_{24},\delta_{24})R(\theta_{14})R(\theta_{23}) \times O(\theta_{13},\delta_{13})R(\theta_{12}). \quad (1)$$

Here, $O(\theta_{ij},\delta_{ij})$ are 4×4 orthogonal matrices with associated phase δ_{ij} in the ij sector, and $R(\theta_{ij})$ are the rotation matrices in the ij sector. Since $\Delta m^2_{41} \sim 1$ eV^2, the oscillations driven by this mass parameter would be averaged out at the far detector of T2HK, T2HKK as well as DUNE. We can see that in this parametrization, the vacuum $\nu_\mu \to \nu_e$ oscillation probability is independent of the θ_{34} mixing angle and the associated phase. However, in the long baseline experiments like DUNE or T2HKK, there are enough matter effects so that this independence is lost and the neutrino appearance probabilities do exhibit a

significant dependence on them at these long baseline experiments [27].

Again, ν_e appearance probability in vacuum contains some terms which are dependent on sine and cosine of δ_{13}, δ_{24} and $(\delta_{13}+\delta_{24})$. These interference terms connecting the mixing angles from both $3+0$ and $3+1$ models, cannot only enhance the amplitude of the probability but also affect the sensitivity of long baseline experiments [27,35]. So keeping this in mind, here we study the effect of this new mass eigenstate at the far detector of these experiments.

III. SIMULATION PROCEDURE

In our analysis we have used GLOBES (Global Long Baseline Experiment Simulator) [36,37] to perform all our computations, along with additional sterile neutrino codes [38,39]. In all the results presented in this paper, we do a full four-generation analysis in the $3+1$ framework and calculate the oscillation probabilities in matter using exact numerical codes. Throughout this analysis we choose the true values of the standard neutrino oscillation parameters as follows [40]:

$$\theta_{12}=33.5^\circ, \qquad \theta_{13}=8.5^\circ,$$
$$\Delta m^2_{21}=7.5\times10^{-5}\ \text{eV}^2, \qquad \Delta m^2_{31}=2.52\times10^{-3}\ \text{eV}^2. \tag{2}$$

We choose true value of $\theta_{23}=45.0^\circ$ for CP violation and mass hierarchy studies, whereas for the octant sensitivity studies we generate data at $\theta_{23}=40.3^\circ$ [we call this case lower octant (LO)] and 49.7° [we call this case higher octant (HO)]. The true mass hierarchy is always taken as normal hierarchy. The true δ_{13} is varied in its full range $[-\pi,\pi]$. Since there are twelve parameters in the $3+1$ scenario, it is impossible to marginalize over all parameters. Therefore, we check the impact of the relevant parameters on each sensitivity study performed in this work and marginalize the resultant χ^2 only over the ones that bring any significant change. We will state clearly our marginalization procedure for every result shown in this paper. Wherever relevant, the marginalization is performed for θ_{13}, θ_{23} and Δm^2_{31} in the ranges are $[7.99^\circ, 8.91^\circ]$, $[38.4^\circ, 53.0^\circ]$ and $[2.40, 2.64]\times10^{-3}$ eV^2 for normal hierarchy (NH) and $[-2.64,-2.40]\times10^{-3}$ eV^2 for inverted hierarchy (IH), respectively.

The issue regarding sterile neutrino mass squared difference and mixing angles is far from settled. While LSND [8,9], MiniBooNE [11–13], gallium [17–21] and reactor anomaly [14–16] require sterile neutrinos mixed with the active ones, the Bugey-3 [41], Daya Bay [42,43], NEOS [44], IceCube [45], MINOS [46] and NOνA [47] experiments are consistent with no active-sterile oscillations and put severe upper limits on the mixing angles θ_{14} [41–43,48], θ_{24} [45] and θ_{34} [46] (see also [47]). The phases are completely unconstrained at the moment. Since there is a certain degree of uncertainty regarding the active-sterile mixing angles, we perform our analysis for two sets of benchmark true values:

$$(\theta_{14},\theta_{24},\theta_{34})=(6.5^\circ,3.5^\circ,12.5^\circ), \tag{3}$$

$$(\theta_{14},\theta_{24},\theta_{34})=(12^\circ,7^\circ,25^\circ), \tag{4}$$

where the former is the set of smaller values of the mixing angles, while the latter are at the higher values. The marginalization over these mixing angles are done in the range $\theta_{14}\le13^\circ$ [42], $\theta_{24}\le7^\circ$ [45] and $\theta_{34}\le26^\circ$ [46]. The phases are taken over their full range $[-\pi,\pi]$. The mass squared difference was taken fixed at $\Delta m^2_{41}=1$ eV^2. The true value of Δm^2_{41} (as well as marginalization over it) has absolutely no impact on our results since the oscillations driven by Δm^2_{41} get effectively averaged as long as they are significantly higher than 10^{-3} eV^2.[2]

IV. EXPERIMENTAL SETUP

A. T2HK

The Hyper-Kamiokande (HK) [5] is the upgradation of the Super-Kamiokande (SK) [50] program in Japan, where the detector mass is proposed to be increased by about 20 times the fiducial mass of SK. The main purpose of this huge detector is to pursue neutrino and proton decay study. The proposed HK consists of two 187 kt water Cherenkov detector modules, near the current SK site, 295 km away and 2.5° off-axis from the J-PARC beam which is currently being used by the T2K experiment [6]. The long baseline experiment T2HK has similar physics goals as DUNE, but being a narrow beam it can be complementary to the DUNE experiment. In this article we will alternately call this setup T2HK or JD × 2 which stands for the two modules of Japan Detector.

For our analysis we have taken a beam power of 1.3 MW and 2.5° off-axis flux. We consider a baseline of 295 km and total fiducial mass of 374 kt (assuming two tanks each of 187 kt). Total run time of 10 years is divided between neutrino and antineutrino mode in 1:3 ratio. For the energy resolution, we assume a Gaussian function of width $15\%/\sqrt{E}$. We have matched the number of events given in Tables II and III of [6]. The signal normalization error in ν_e ($\bar{\nu}_e$) appearance and ν_μ ($\bar{\nu}_\mu$) disappearance channel are 3.2% (3.6%) and 3.9% (3.6%), respectively. The background and energy calibration error in all the channels are 10% and 5%, respectively.

[2]Recently, in [49], the authors have put strong constraints on the sterile mixing angles from global analysis. The upper limit, used in this work for θ_{34}, is far outside the range specified in [49]. But we have explicitly checked our results with the new constraint on θ_{34} and found that the results reported in this work will not change by 5%.

B. T2HKK

In [6], the collaboration has discussed the possibility of shifting the second detector module of the HK setup to Korea. Thus, the T2HKK experiment will have two sets of detectors; one at the HK site at a baseline of 295 km and the other one at Korea at a baseline of ∼1100 km. The second detector module will be a 187 kt water Cherenkov detector identical to the HK detector module in Kamioka. The second oscillation maximum takes place near $E_\nu = 0.6$ GeV at the ∼1100 km baseline. If the detector is placed at 2.5° of axis, the peak energy of the narrow beam coincides with the second oscillation maximum at 0.6 GeV. We will refer to this setup alternately as T2HKK or JD + KD which implies one detector at Japan while the other at Korea. The background and systematic uncertainties are kept the same as T2HK.

C. DUNE

DUNE (Deep Underground Neutrino Experiment) [1–4] is a future long baseline experiment which is supposed to address all three important issues in the neutrino sector—determination of neutrino mass hierarchy, leptonic *CP* violation, and the octant of θ_{23}. The neutrino beam source will be at Fermilab in Chicago, IL, and the far detector will be at Sanford Underground Research Facility (SURF) in South Dakota, at a distance of 1300 km from the beam source. The accelerator facility at Fermilab will give a proton beam of energy 80–120 GeV at 1.2–2.4 MW. The proton beam will eventually give a wide neutrino beam of energy range 0.5–8.0 GeV which will be detected at the far site. The far site will consist of four identical detectors of about 10 kt each. The detector will be a liquid argon time projection chamber (LArTPC).

In our analysis, we have assumed that a liquid argon (LAr) detector of fiducial mass 34 kt will be installed at a baseline of 1300 km and the 120 GeV–1.2 MW proton beam will deliver 10^{20} protons on target per year. We assume total run time of ten years which is equally divided between neutrinos and antineutrinos and this will give a total exposure of 35×10^{20} kt-POT-yr. The energy resolution considered here for μ and e are $20\%/\sqrt{E}$ and $15\%/\sqrt{E}$, respectively. We have combined both ν_e appearance and ν_μ disappearance channels, both in neutrino and antineutrino mode. The signal efficiency is taken to be 85%. All other backgrounds are taken from [3]. In the ν ($\bar{\nu}$) mode, the signal normalization error is 2% (5%), the background normalization error is 10% (10%) and the energy calibration error is 5% (5%). The choice of systematics is conservative compared to the projected systematics in [3].

In Table I, we give the total number of expected events for all channels in all three experiments for both the 3 + 0 and the 3 + 1 scenarios. The value of all the phases have been taken as zero, while $\theta_{23} = 45°$. The values of the other oscillation parameters used have been given before in Sec. III. For both JD and KD we divide the total run time of ten years in the ratio of 1:3 between ν and $\bar{\nu}$, while in DUNE the ratio is 1:1. The events in the 3 + 1 case is generated for the smaller set of mixing angles given in Sec. III.

TABLE I. Total number of events in JD, KD and DUNE in both scenarios. In the 3 + 0 case, we take $\delta_{13} = 0°$ while in the 3 + 1 case, all three phases are taken as zero. For both JD and KD we divide the total run time of ten years in the ratio of 1:3 between ν and $\bar{\nu}$, while in DUNE the ratio is 1:1. The events in the 3 + 1 case is generated for the smaller set of mixing angles given in Sec. III. We take $\theta_{23} = 45°$ for all cases. The values of the other oscillation parameters taken are given in Sec. III.

Experiments	Channels	3 + 0	3 + 1
JD	$\nu_e(\bar{\nu}_e)$ app	1839 (1715)	1865 (1738)
	$\nu_\mu(\bar{\nu}_\mu)$ disapp	10478 (14435)	10390 (14345)
KD	$\nu_e(\bar{\nu}_e)$ app	132 (165)	134 (169)
	$\nu_\mu(\bar{\nu}_\mu)$ disapp	1373 (1477)	1357 (1437)
DUNE	$\nu_e(\bar{\nu}_e)$ app	1101 (284)	1146 (296)
	$\nu_\mu(\bar{\nu}_\mu)$ disapp	7419 (5086)	7326 (5054)

V. RESULTS

A. Numerical probabilities

In this section we present some of our results at the probability level in order to understand the physics potential of these experiments. Figure 1 gives the bi-probability plots for JD (the Japan detector at 295 km) at its first oscillation maximum at 0.5 GeV and KD (the Korean detector at 1100 km) at its second oscillation maximum at 0.66 GeV. For each case we have considered all the four combinations of octant [higher octant (HO) or lower octant (LO)] and mass hierarchy [normal hierarchy (NH) or inverted hierarchy (IH)] i.e., NH-LO (red), IH-LO (blue), NH-HO (green) and IH-HO (black). As stated before, for LO we have chosen $\theta_{23} = 40.3°$ as the benchmark value and for HO we take $\theta_{23} = 49.7°$. For NH we have chosen $|\Delta m^2_{31}| = 2.457 \times 10^{-3}$ eV^2 and for IH we have chosen $|\Delta m^2_{31}| = 2.449 \times 10^{-3}$ eV^2. The effect of the variation in the bi-probability plots due to the sterile sector phases δ_{24} and δ_{34} varying in their $[-\pi, \pi]$ range is shown by the shaded regions. For comparison we also show the bi-probability ellipse for the standard 3 + 0 case by the solid curves of the same color.

The top-left panel shows that for JD there is a strong overlap for NH and IH bi-probability curves even for the 3 + 0 case and for both LO and HO. This reflects the fact that JD has a smaller baseline and energy and hence small matter effects. As a result, the sensitivity of JD to *CP* violation is expected to suffer from mass hierarchy degeneracy. As we switch on the sterile neutrino mixing, the sharp bi-probability lines start to spread and there is a whole band of bi-probabilities coming from the fact that now in addition to δ_{13} there are two additional phases δ_{24} and δ_{34}. The bi-probability bands for the different colors representing different cases start to overlap more with each

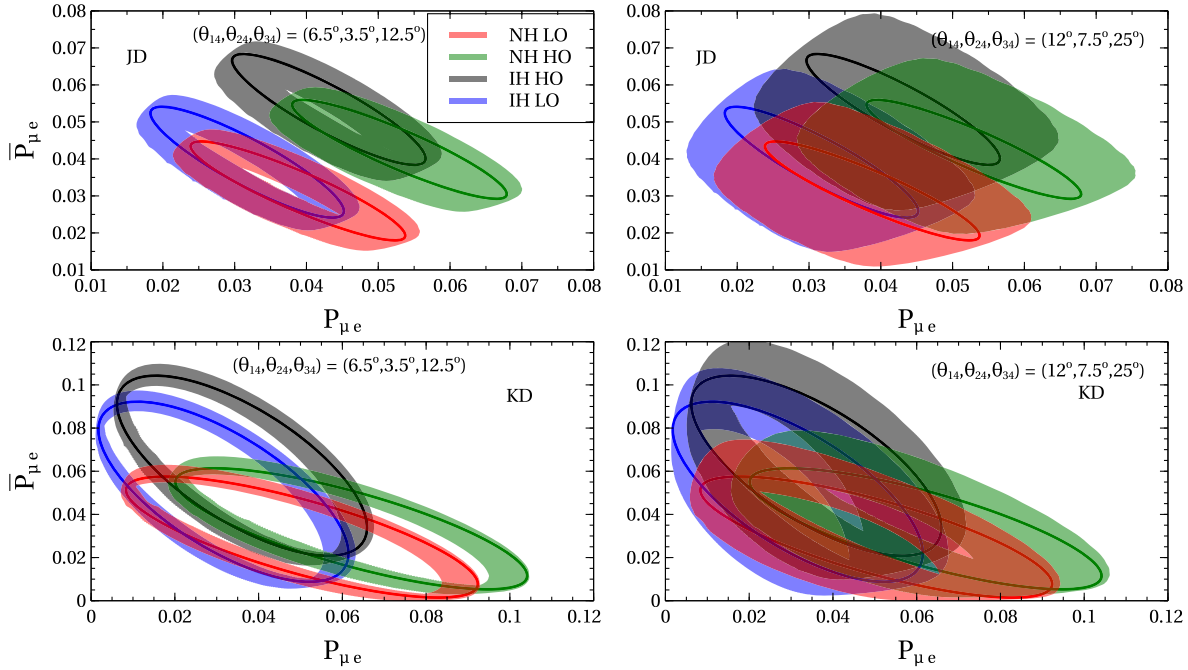

FIG. 1. $P_{\mu e}$ vs $\bar{P}_{\mu e}$ bi-probability plots for JD and KD. The first row shows the plots for JD (295 km and $E = 0.5$ GeV) and the second row shows the plots for KD (1100 km and $E = 0.66$ GeV). The left column is for the lower set of sterile mixing angles and the right column is for the higher set of sterile mixing angles. The shaded regions show the variation of the bi-probability when the sterile phases δ_{24} and δ_{34} are varied within $[-\pi,\pi]$. The solid curves describe the $3 + 0$ case. The different colors correspond to different combinations of mass hierarchy and the octant of θ_{23}.

other. The overlap increases significantly as we increase the sterile mixing angles, shown in the top-right panel, owing to the fact that the effect of the phases δ_{24} and δ_{34} increase. The corresponding bi-probability results for the KD baseline and peak energy of 0.66 GeV is shown in the lower panels. As for JD, the bi-probability curves for $3 + 0$ overlap between the different hierarchies even for KD, but the overlap is less. As we switch on the sterile mixing angle (bottom-left panel) the bi-probability lines blur into a band, though the spread in the case of KD appears to be slightly less. As the sterile mixing angles increase (bottom-right panel) the blurring increases showing the increased effect of the phases associated with the sterile mixing angles. We have checked that the main contribution to the blurring of the bi-probability plot comes from the phase δ_{24}. The effect of δ_{34} is subdominant, although nonzero.

Here in Fig. 2, we show the CP violation in terms of an asymmetry defined at the probability level to provide some additional insight. We define the CP asymmetry as

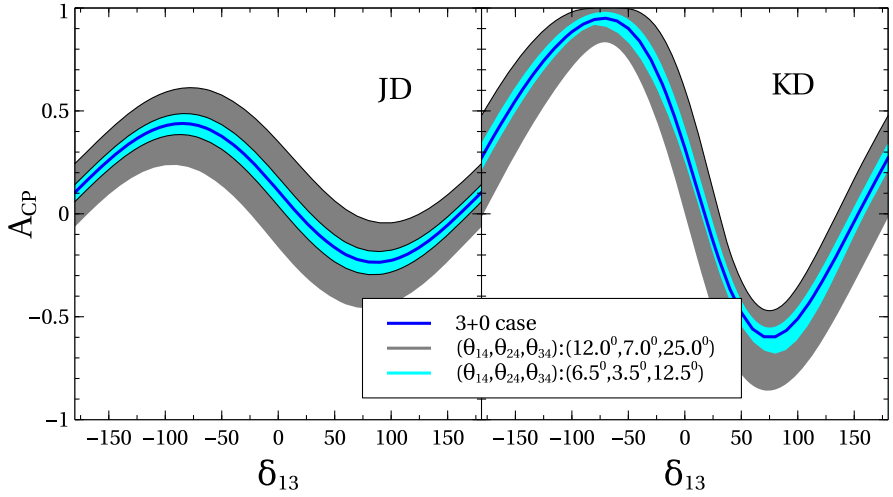

FIG. 2. CP asymmetry at JD (left) and KD (right). The bands represent the variation of δ_{24} and δ_{34}.

$$A_{CP} = \frac{P_{\mu e} - \bar{P}_{\mu e}}{P_{\mu e} + \bar{P}_{\mu e}}. \quad (5)$$

The left panel of Fig. 2 shows the CP asymmetry as a function of δ_{CP} for the JD baseline of 295 km and at a fixed energy 0.5 Gev which corresponds to the first oscillation maximum at this baseline. The right panel shows the CP asymmetry for the KD baseline of 1100 km and at a fixed energy of 0.66 GeV which corresponds to the second oscillation maximum for this baseline. The solid blue curves depict the A_{CP} for the $3+0$ ν case in both panels. The bands represent the effect of the sterile phases. For each δ_{13}, the bands show the range of A_{CP} for the full range of values of δ_{24} and δ_{34} between $[-\pi, \pi]$. The cyan bands show the effect of the sterile phases for the lower set of sterile mixing angles and the grey bands show the same for the higher set of mixing angles. We see that the presence of the sterile neutrino mixing spreads the A_{CP} in both sides of the standard $3+0$ case. This implies that for a given true value of δ_{13}, the CP asymmetry in the presence of sterile neutrinos could either increase or decrease for both JD and KD baselines and energies, depending on the true values of a δ_{24} and δ_{34}. Looking from another angle, this also implies that the presence of sterile neutrino mixing brings in an uncertainty in the expected CP asymmetry at long baseline experiments. Observation of a certain CP asymmetry signal in the data could come from degenerate solutions involving mixing angles and phases in the $3+0$ sector and the sterile sector. We can also see from the plots that with higher mixing, widths of the bands increase and hence the uncertainties in the CP sector introduced by the sterile phases increase. We also note that the CP asymmetry is significantly higher for KD than for JD. The reason is that the shape and magnitude of the curves largely depend on the baseline and energy value chosen, or more precisely on the L/E factor.

Figure 3 shows the MH asymmetry for JD (left) and KD (right) baselines at fixed energies of 0.5 and 0.66 GeV, respectively. The MH asymmetry is defined as

$$A_{MH} = \frac{P_{\mu e}^{NH} - P_{\mu e}^{IH}}{P_{\mu e}^{NH} + P_{\mu e}^{IH}}. \quad (6)$$

In NH we have taken $\Delta m^2_{31} = 2.45 \times 10^{-3}$ eV^2 while in IH we have taken $\Delta m^2_{31} = -\Delta m^2_{31} + \Delta m^2_{21}$. Just as in the previous figure, the blue solid curves show the MH asymmetry for the standard $(3+0)$ case. As before the bands are obtained when the sterile mixing angles δ_{24} and δ_{34} are varied in their full range $[-\pi, \pi]$. The cyan bands are for the lower set of sterile mixing angles and the grey bands are for the higher set of sterile mixing angles. From Fig. 3, we can see the effect of the new physics at the probability level. We can see naively that at the probability level it appears that for the $3+1$ scenario, the mass hierarchy asymmetry has a chance of either increasing or decreasing compared to its $3+0$ expected reach, depending on the true values of δ_{24} and δ_{34}. We can see that with the increase of the sterile mixing angles the effect increases. As in Fig. 2, we find that the MH asymmetry expected in KD is more than in JD and the reason for this is its higher chosen energy value and earth matter effects.

B. Statistical χ^2

We define the χ^2 (statistical) as follows:

$$\chi^2(n^{\text{true}}, n^{test}, f) = 2\sum_i^{\text{bins}} \left(n_i^{\text{true}} ln \frac{n_i^{\text{true}}}{n_i^{\text{test}}(f)} + n_i^{\text{test}}(f) - n_i^{\text{true}} \right) + f^2, \quad (7)$$

where n_i^{true} and n_i^{test} are the event rates that correspond to data and fit in the ith bin and f represents the nuisance parameters. For JD, KD and DUNE, we have 24, 10 and 39

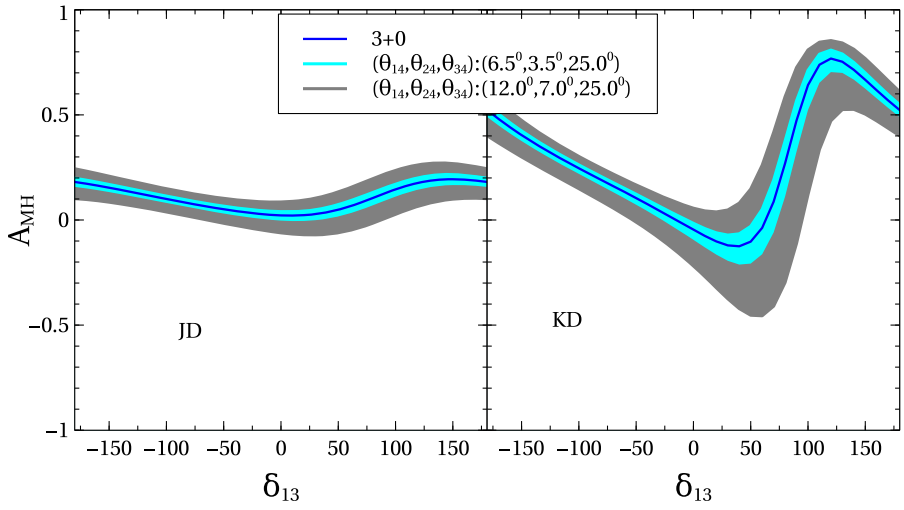

FIG. 3. MH-asymmetry as a function of δ_{13} for JD(left) and KD(right). The bands represent the variation of δ_{24} and δ_{34}.

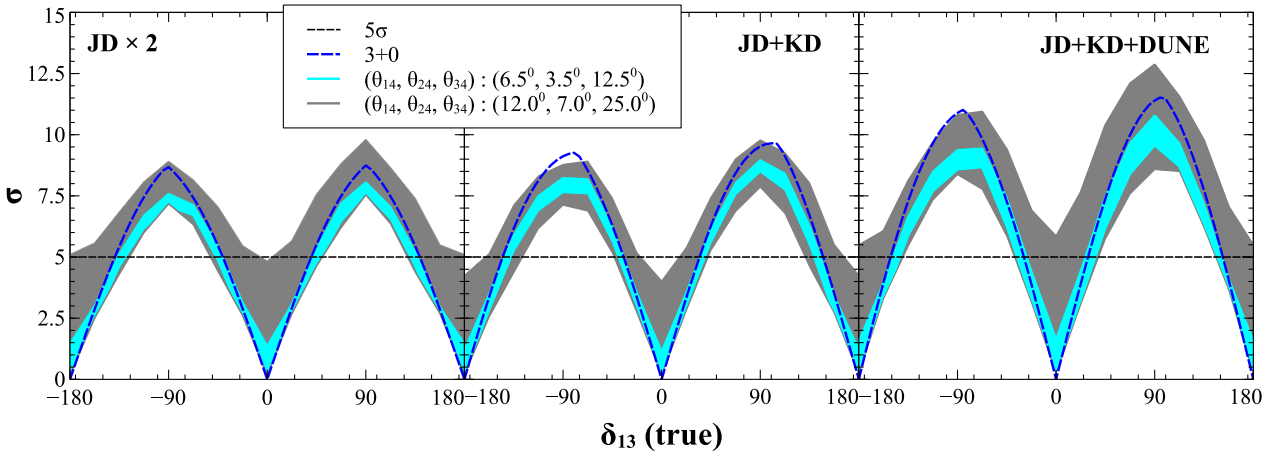

FIG. 4. The expected *CP* violation sensitivity of T2HK (JD × 2), T2HKK (JD + KD) and DUNE + JD + KD under the assumption that we do not know the source of its violation. The bands correspond to variation of δ_{24} and δ_{34} in the true parameter space. The results are for true normal hierarchy.

bins, respectively. Here in this definition, n^{test} changes according to the sensitivity studied for a particular model. We have marginalized over the systematic uncertainties for each experiment as given in Sec. IV.

C. *CP* sensitivity

In this section, we present our *CP* violation sensitivity results in the presence of a light sterile neutrino. That is, we are addressing the following question: If *CP* is violated in Nature, then at what C.L., T2HK (JD × 2) and T2HKK (JD + KD) can exclude the *CP* conserving scenarios in the presence of a sterile neutrino? In the 3 + 1 scenario, we have two more phases θ_{24} and θ_{34} in addition to the standard *CP* phase δ_{13}. So while studying *CP* violation sensitivity of these experiments in the presence of sterile neutrinos, we consider the following two situations:

(1) *CP* is violated and we do not know the source of its violation. That is, it can be due to any of the three phases.
(2) *CP* is violated and we know the source of its violation. For instance, say we assume that it is due to the standard Dirac *CP* phase δ_{13}.

As explained above, we have presented our results for two sets of sterile mixing angles and for each set we fix the standard oscillation parameters to their best fit values in "data" and vary all three true phases in their full range $[-\pi, \pi]$. While answering the question of *CP* violation in the first scenario, we generate the data at a given true value of δ_{13}, δ_{24} and δ_{34} and calculate the $\Delta\chi^2_{\text{min}}$ by considering all eight possible *CP* conserving scenarios in the "fit." We marginalize over a fine grid of θ_{14}, θ_{24}, θ_{34} in their allowed range in the fit. In addition, we have marginalized over the test θ_{13} in its 3σ allowed range.

The results of *CP* violation sensitivity in the first scenario are presented in Fig. 4. The mass hierarchy is kept fixed as NH in both the data as well as the fit for this figure and in the next two figures in this subsection. The blue dashed line corresponds to the standard *CP* sensitivity in the 3 + 0 case as a function of $\delta_{13}(\text{true})$. The bands correspond to the 3 + 1 case with all possible choices for the other two phases $\delta_{24}(\text{true})$ and $\delta_{34}(\text{true})$. The thinner cyan band gives this band for $\delta_{24}(\text{true})$ and $\delta_{34}(\text{true})$ when the sterile mixing angles are taken to be at their smaller benchmark value while the grey band is obtained for the corresponding case when the sterile mixing angles are kept at their limiting benchmark value. In both cases these are the value of the sterile mixing angles in the data, kept fixed in the entire band, while in the fit they are marginalized as discussed above. We observe that for all $\delta_{13}(\text{true})$ which give more than 5σ *CP* sensitivity, the cyan band almost lies below the blue line. So for relatively small 3 + 1 mixing angles, sensitivity to *CP* violation in the 3 + 1 case decreases compared to the standard 3 + 0 case. But as the mixing angles increase, the 3 + 1 grey band spans both sides of the 3 + 0 plot. In the 3 + 1 case, as discussed in [35], there are two effects that come into play. First, the number of parameters to be marginalized in the fit is higher than the 3 + 0 case and marginalizing over a large number of parameters brings the χ^2_{min} down. Second, the effect of the variation of the true phases changes with the variation of the true values of the mixing angles. When mixing angles are small, the effect of the true phases is also small and hence the first effect dominates the second one. As a result, χ^2_{min} decreases compared to the 3 + 0 case. But as the true mixing angles increase, the effect of the variation of the true phases increases simultaneously and as a result the width of the grey band increases. So for higher values of the mixing angles, the second effect tends to increase the χ^2_{min} and as a result overall sensitivity increases and the grey band spreads on both sides of the 3 + 0 plot.

As seen from Fig. 4, T2HKK (JD + KD) has slightly better sensitivity to *CP* violation in the 3 + 0 case than T2HK (JD × 2). But in the 3 + 1 case, we observe that

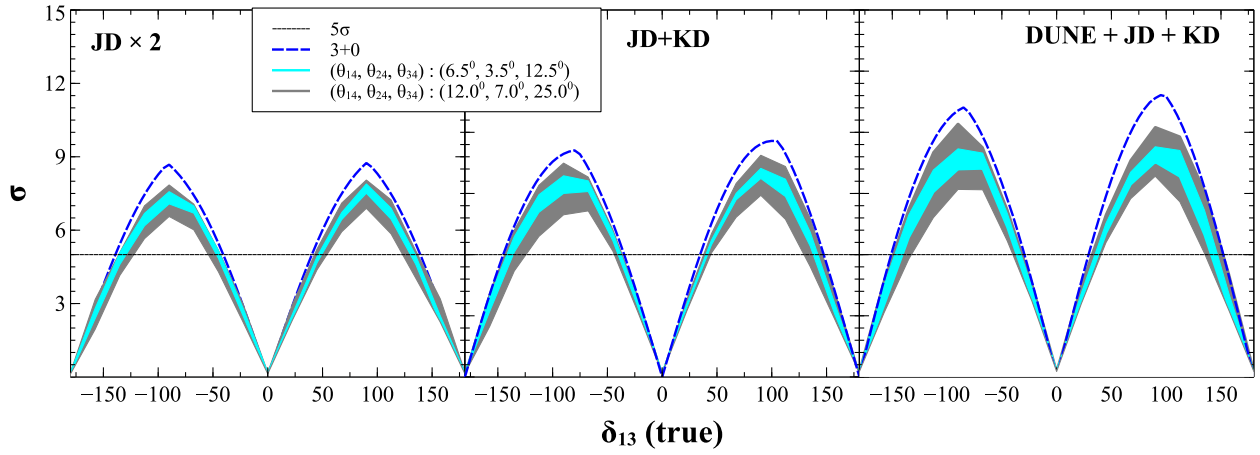

FIG. 5. The expected *CP* violation sensitivity of T2HK (JD × 2), T2HKK (JD + KD) and DUNE + JD + KD under the assumption that we know the source of its violation and it is due to δ_{13}. The bands correspond to variation of δ_{24} and δ_{34} in the true parameter space. The results are for true normal hierarchy.

T2HK and T2HKK have almost equal sensitivity to *CP* violation at $\delta_{13} = \pm\pi/2$ when mixing angle are large. But for smaller mixing angles, T2HKK gives slightly better sensitivity than T2HK (JD × 2). Also note that in the 3 + 1 case, we have nonzero *CP* violation sensitivity even at the *CP* conserving values of δ_{13}(true). For the higher mixing angle case and for δ_{13}(true) = 0 or $\pm\pi$, we have more than 3σ *CP* violation sensitivity for δ_{24}(true) in the range $[45°, 135°]$ and $[-135°, -45°]$. The effect of δ_{34}(true) is less important. Combining JD and KD with DUNE enhances the *CP* violation sensitivity and we observe that even when δ_{13}(true) = 0 or $\pm\pi$, it is possible to achieve more than 5σ *CP* violation sensitivity in the higher mixing angle case for δ_{24}(true) in the range $[90°, 112°]$ and $[-112°, 90°]$. Again the impact of δ_{34} is not important.

To address the second scenario we consider the *CP* conserving cases for δ_{13} alone in the fit while we have marginalized over the two new phases δ_{24} and δ_{34} in the allowed 3σ range. All other 3 + 1 mixing angles and θ_{13} are marginalized as explained above. The results are shown in Fig. 5, where we observe that the *CP* violation sensitivity in the 3 + 1 case decreases compared to the standard 3 + 0 sensitivity in all three experimental setups. Both the cyan and grey bands lie below the 3 + 0 sensitivity plot for all true δ_{13}. We also observe that the minima of the grey band is nearly at the same level in T2HKK and DUNE + T2HKK while it is slightly lower in the case of T2HK. From Fig. 5 (Fig. 6), we observe that restricting the source of *CP* violation to only δ_{13} (δ_{24}) in the fit brings down the sensitivity. In the previous case (Fig. 4), we have considered only eight combinations of the phases in the fit while in this case we have marginalized over two phases in their full allowed range. Marginalizing over a large number of parameters lead to decrease in sensitivity.

In Fig. 6, we have shown the results for *CP* violation due to δ_{24} and here the width of the bands is due to the variation

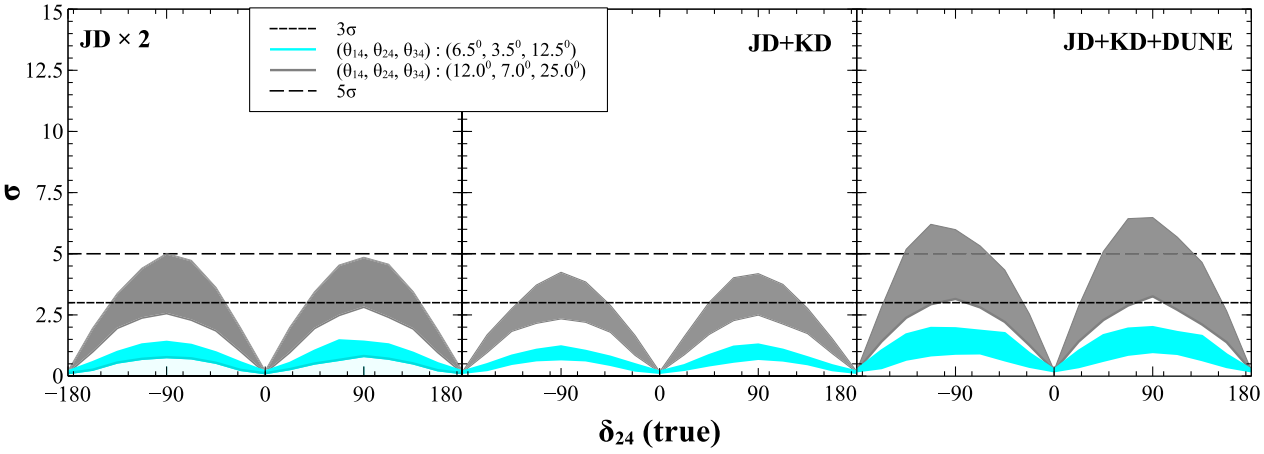

FIG. 6. The expected *CP* violation sensitivity of T2HK (JD × 2), T2HKK (JD + KD) and DUNE + JD + KD under the assumption that we know the source of its violation and it is due to δ_{24}. The bands correspond to variation of δ_{13} and δ_{34} in the true parameter space. The results are for true normal hierarchy.

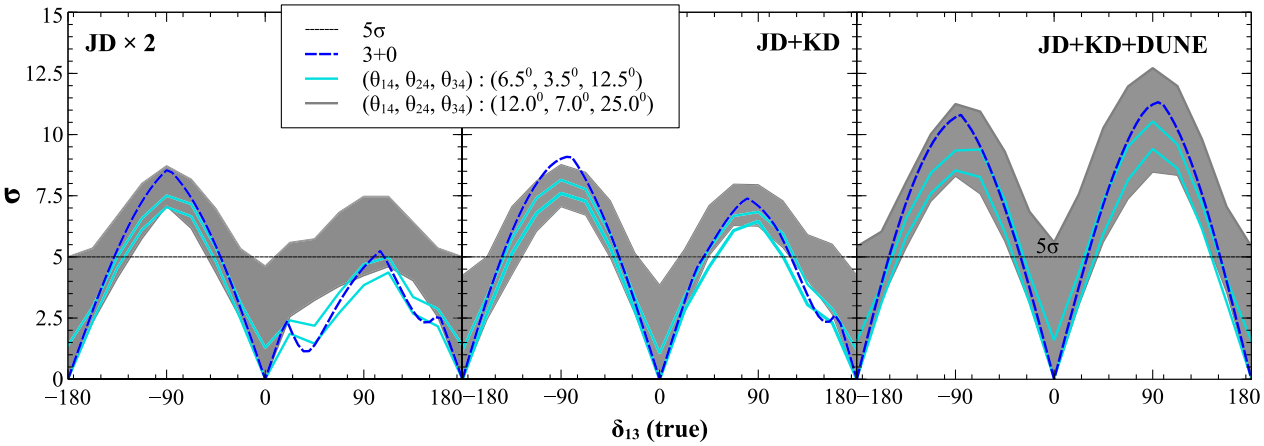

FIG. 7. The expected *CP* violation sensitivity of T2HK (JD × 2), T2HKK (JD + KD) and DUNE + JD + KD under the assumption that we do not know the source of its violation as well as the hierarchy. The bands correspond to variation of δ_{24} and δ_{34} in the true parameter space. The results are for true normal hierarchy.

of $\delta_{13}(\text{true})$ and $\delta_{34}(\text{true})$ in their full allowed range. Also in the fit we have marginalized over these two phases in their full range and choose *CP* conserving values for δ_{24}. *CP* violation sensitivity in this case is much lower than the previous two cases and the two bands are well separated from each other. So if there is a sterile neutrino and *CP* violation is considered to be solely due to δ_{24}, then T2HK and T2HKK can measure it at 3σ C.L. only for some fraction of true δ_{24} and as seen from Fig. 6, T2HK is better than T2HKK. Even after combining with DUNE, we can achieve 5σ *CP* violation sensitivity for some fraction of true δ_{24} only around the peak when the mixing angles are large.

1. CP violation sensitivity if hierarchy is unknown

The results presented in the previous section are under the assumption that the mass hierarchy will be known by the time of operation of these experiments. We have also checked the *CP* violation sensitivity for the true inverted hierarchy and the behaviors of the results are consistent.

In this section we show the *CP* violation sensitivity in the $3 + 1$ case without fixing the mass hierarchy to its true case in the fit. In Fig. 7 we show the results for expected *CP* violation sensitivity for the first scenario where we rule out *CP* conserving values of all the three phases and with marginalization over MH in the fit. We have assumed the NH to be true in this figure. That is, for each "simulated data" case we find the χ^2 for eight combinations of *CP* conserving phases for each hierarchy in the fit and hence sixteen combinations in total. The minimum $\Delta\chi^2_{\text{min}}$ amongst these sixteen combinations are plotted in Fig. 7 as a function of $\delta_{13}(\text{true})$ where the full range of $\delta_{24}(\text{true})$ and $\delta_{34}(\text{true})$ are represented in the bands. Marginalization over other parameters is the same as explained in the previous subsection. The regions between the two cyan lines represent the *CP* violation sensitivity for the small mixing angles benchmark point, while the grey band depicts the sensitivity for the higher mixing angles benchmark case. The blue dashed lines show the $3 + 0$ sensitivity for each of the three experimental setups. We observe that in the $3 + 0$ scenario, *CP* violation sensitivity decreases significantly for T2HK, especially in the upper half plane (UHP) $[\delta_{13}(\text{true}) > 0]$ if the MH is taken to be unknown. For T2HKK although there is a drop in the sensitivity in the UHP for the $3 + 0$ case compared to its counterpart in Fig. 4, the effect of marginalizing over hierarchy is less here than for T2HK. This happens because KD can resolve the mass hierarchy degeneracy to a large extent in the T2HKK setup. Once we combine DUNE with T2HKK, the effect of the unknown hierarchy almost vanishes. On the other hand in the presence of a sterile neutrino, the *CP* violation sensitivity decreases if the new mixing angles are small. But for the larger mixing angles case, the sensitivity increases in the UHP and for some combinations of $\delta_{24}(\text{true})$ and $\delta_{34}(\text{true})$, we can have more than 5σ sensitivity at $\delta_{13} = +\pi/2$ for T2HK. Adding DUNE not only enhances the sensitivity but also nullifies the effect of unknown MH even in the presence of a sterile neutrino.

D. Mass hierarchy sensitivity

In this section, we discuss the expected sensitivity to neutrino mass hierarchy of T2HK and T2HKK in the $3 + 1$ scenario. For that we generate the data at a given true MH and fit it with the wrong hierarchy. We marginalize over all the three phases in the fit and all the sterile mixing angles and also $|\Delta m^2_{31}|$ and $\sin^2\theta_{23}$. Here we have not marginalized over θ_{13} due to computational challenges. We have seen in Fig. 3 that the MH asymmetry can change due to the presence of sterile neutrino mixing. However, there we have done everything only at the probability level and for fixed values of oscillation parameters as well as for a fixed energy. We will now show how the expected sensitivity to MH changes due to sterile neutrinos from a full analysis of

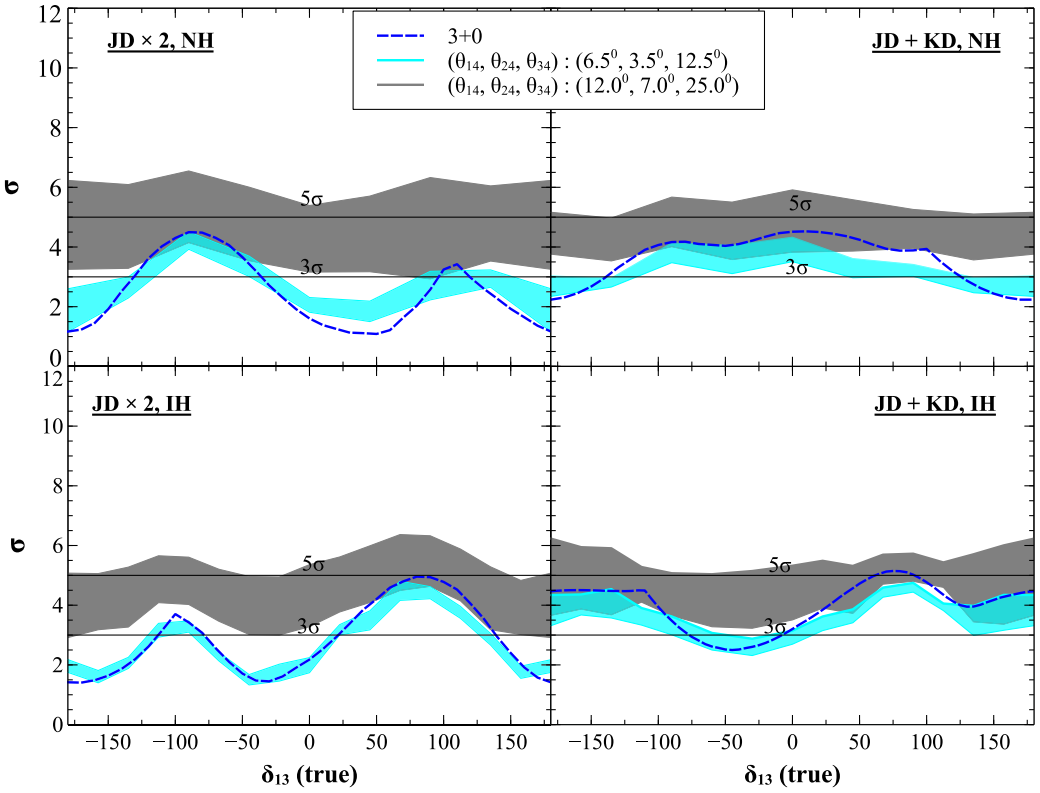

FIG. 8. The expected mass-hierarchy sensitivity of T2HK (JD × 2) and T2HKK (JD + KD). The upper panel is for true NH while the lower panel is for true IH. The bands correspond to the variation of the sterile phases in the true parameter space.

expected data, when one takes all relevant marginalization into account.

The results for T2HK and T2HKK for both NH (upper panel) and IH (lower panel) as true are shown in Fig. 8. The presentation and description of the bands are the same as that in the previous subsection. We observe that the sensitivity to mass hierarchy in the presence of a sterile neutrino changes significantly in both experiments. We have explicitly checked the effect of marginalization on mass hierarchy sensitivity. Here also, we notice the two features discussed in Sec. V B. We observe that

(1) For the higher sterile mixing angles, the impact of the variation of the true phases increases and it tends to increase the $\chi^2_{\rm min}$.
(2) Effect of marginalization over test $|\Delta m^2_{31}|$ in the wrong hierarchy is very important for the MH sensitivity study. Its effect is seen to be the most for the $3+0$ case and keeps decreasing with the strength of the true sterile mixing. As a result the $\chi^2_{\rm min}$ goes up for the higher set of sterile mixing angles.

For smaller sterile mixing angles, we observe that the width of the cyan band is small in both hierarchies and the sensitivity for the $3+1$ scenario in this case is nearly the same as $3+0$. In the case of T2HK, the cyan band swings around the $3+0$ plot but in T2HKK, it lies below the $3+0$ line for most of the $\delta_{13}(\text{true})$ values, in both hierarchies. However, the mass hierarchy sensitivity seems to increase for the larger mixing angle case. This apparently appears counterintuitive to what we have observed in Fig. 1 where the overlap between the bi-probability plots was seen to increase when we increased the sterile mixing angles, making it appear as though the sensitivity to mass hierarchy would decrease as the sterile mixing angle was increased. We can also note that in Fig. 8 the grey band does not span equally on both sides of the cyan band. Instead the two bands get separated for most values of $\delta_{13}(\text{true})$. This again appears to be in contrast to Fig. 3 where the cyan band was embedded nearly symmetrically inside the grey band. The reason for both these apparent conflicts can be traced back to the impact of marginalization of the mass hierarchy χ^2 over $|\Delta m^2_{31}|$. We have checked that the marginalization over $|\Delta m^2_{31}|$ alone reduces the mass hierarchy χ^2 by nearly an order of magnitude for the $3+0$ scenario. For the smaller sterile mixing angle case, the effect of sterile neutrino parameters is less and the final marginalized χ^2 is close to what we have for the $3+0$ case. However, as the sterile mixing angle is increased the effect of marginalization over $|\Delta m^2_{31}|$ is able to reduce the χ^2 relatively less and as a result the final mass hierarchy sensitivity appears to rise. For the same reason the cyan band becomes asymmetric with respect to the grey band. For the largest sterile mixing angle case we have more than 5σ sensitivity for mass hierarchy for any $\delta_{13}(\text{true})$.

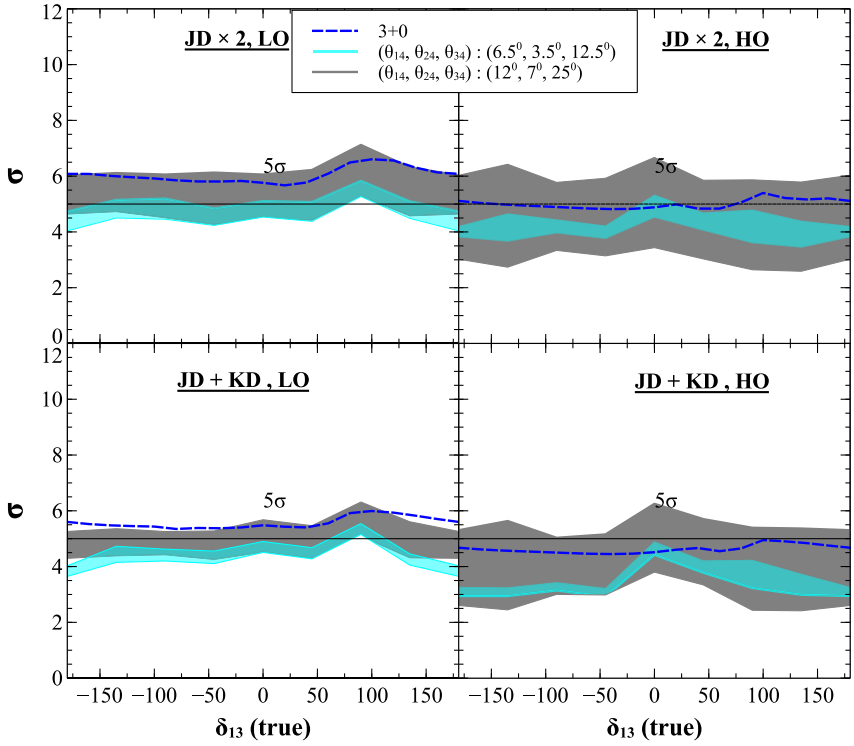

FIG. 9. The expected octant discovery potential of T2HK (JD × 2) and T2HKK (JD + KD). In the LO (HO), we consider $\theta_{23} = 40.3°$ (49.7°) as the true value. The upper panel is for T2HK (JD × 2) while the lower panel is for T2HKK (JD + KD). The bands correspond to the variation of the sterile phases.

E. Octant discovery

In this section, we study the octant discovery potential of T2HK and T2HKK in the 3 + 1 scenario. We also present a combined analysis of T2HKK with DUNE. We consider the same benchmark value of true θ_{23} for which we have shown the bi-probability plots in Fig. 1. We then show the potential of these experiments to exclude the wrong octant for the two sets of sterile mixing angles. In data, we vary all three phases, as discussed above, we show the band of $\Delta\chi^2_{\text{min}}$ as a function of the $\delta_{13}(\text{true})$. The band corresponds to the full range of $\delta_{24}(\text{true})$ and $\delta_{34}(\text{true})$. In the fit, we marginalize over the sterile mixing angles and the phases in their allowed ranges. In addition, we marginalize over θ_{13} and for a true LO (HO), θ_{23} is marginalized in the HO (LO). We consider the full 3σ allowed range for both θ_{13} and θ_{23}. We show the results only for the assumed true normal mass hierarchy.

From Fig. 9, we observe that the potential of T2HK to exclude the wrong octant is slightly higher than for

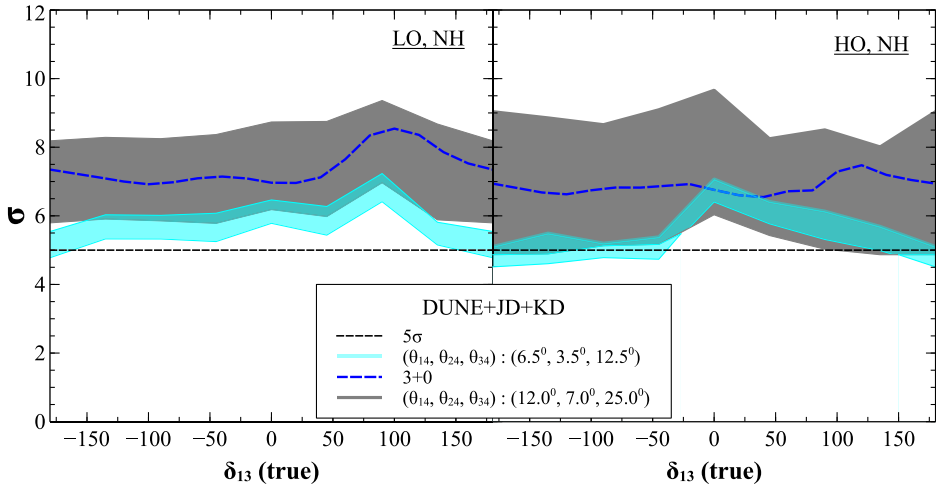

FIG. 10. The octant discovery potential of DUNE + T2HKK (JD + KD).

T2HKK. If LO is the true octant in the standard 3ν scenario, then both T2HK and T2HKK can exclude the wrong HO at 5σ for all $\delta_{13}(\text{true})$. However for true HO, excluding the LO is not possible at 5σ for all $\delta_{13}(\text{true})$, though the expected sensitivity reach is seen to remain high. In the presence of a sterile neutrino, the expected sensitivity gets modified and we observe that for small sterile mixing, the potential to exclude the wrong HO is significantly less than the standard $3+0$ case. For large mixing angles, the width of the band increases and for some combinations of $\delta_{24}(\text{true})$ and $\delta_{34}(\text{true})$, the grey band slightly crosses the $3+0$ plot for some fraction of $\delta_{13}(\text{true})$. On the other hand for true HO, the standard $3+0$ plot lies within the grey band while the cyan band lies below it except for some small fraction of $\delta_{13}(\text{true})$ around zero. Also, one can note that for large sterile mixing angles, some combinations of the new phases give more than 5σ HO discovery potential for both setups.

If we add DUNE with T2HKK (Fig. 10), the octant discovery potential changes significantly. For large (small) sterile mixing angles, if LO is the true octant, then it is possible to exclude the HO at 5σ for all $\delta_{13}(\text{true})$ [all $\delta_{13}(\text{true})$ except some fraction around $\delta_{13}(\text{true}) = \pm\pi$], irrespective of the true values of the other two phases. Even in the case of true HO, we can rule out the LO at 5σ C.L. except for some fraction of $\delta_{13}(\text{true})$.

VI. SUMMARY AND CONCLUSION

The final word on existence or nonexistence of sterile neutrino oscillations is yet to be affirmatively answered. The LSND hint for $\bar{\nu}_\mu \to \bar{\nu}_e$ oscillations as well as the reactor and gallium experiment anomalies demand that there be an extra light neutrino state which must be sterile with $\Delta m^2 \sim 1\ \text{eV}^2$ and mixed the active neutrino, albeit weakly. The presence of the mixed sterile state brings in additional mixing angles and phases that affect the oscillation probabilities at long baseline experiments. In particular, while the additional mass squared difference drops out due to averaging of the fast oscillations at the long baselines, all three active-sterile mixing angles θ_{14}, θ_{24} and θ_{34} and the two additional phases δ_{24} and δ_{34} impact the neutrino oscillation probabilities. The active-sterile mixing angles θ_{14}, θ_{24} and θ_{34}, even though constrained by data from Daya Bay, IceCube and MINOS, respectively, bring in additional uncertainty in the oscillation probabilities, while the new phases δ_{24} and δ_{34} are totally unconstrained. Hence the *CP* violation sensitivity is obviously affected, with the possibility of additional *CP* violation coming from the new phases δ_{24} and δ_{34}. The mass hierarchy sensitivity and the octant sensitivity also get affected.

In this work we studied the impact of this active-sterile mixing angles and new phases on the physics reach of the T2HK and T2HKK proposals. We also studied the combined sensitivity reach of T2HKK and DUNE. We showed the impact of the sterile mixing angles and phases on T2HK and T2HKK using the bi-probability plots. We further illustrated the expected *CP* violation sensitivity for T2HK and T2HKK by plotting the *CP* asymmetry as well as the mass hierarchy asymmetry as a function of the standard *CP* phase δ_{13} while the sterile phases δ_{24} and δ_{34} were allowed to vary in the full range. In all cases we showed the corresponding line for the standard $3+0$ case in order to illustrate the change brought by the $3+1$ scenario. As expected these plots showed that the spread in the sensitivity due to the sterile sector increased as the sterile mixing angles increased.

We showed the expected *CP* violation sensitivity of T2HK and T2HKK, and the combined *CP* reach of T2HKK+DUNE as a function of $\delta_{13}(\text{true})$, while $\delta_{24}(\text{true})$ and $\delta_{34}(\text{true})$ were allowed to take any value in their full range $[-\pi, \pi]$ and the corresponding band was plotted. This study was performed first by checking against *CP* conserving cases for all three phases δ_{13}, δ_{24} and δ_{34} in the fit and then by checking only against the *CP* conserving cases for δ_{13} and marginalizing over the others. It was shown that while in the latter case it might appear that the *CP* violation sensitivity of the experiment is going down, in the former more general case the sensitivity might even increase over that expected for the $3+0$ case for some value of $\delta_{24}(\text{true})$ and $\delta_{34}(\text{true})$. The combined T2HKK+DUNE data could give us a *CP* violation sensitivity of more than 12.5σ for certain values of $\delta_{24}(\text{true})$ and $\delta_{34}(\text{true})$ and $\delta_{13}(\text{true}) = \pi/2$. Also, even for $\delta_{13}(\text{true}) = 0°$ we can get a greater than 5σ sensitivity for *CP* violation from the combined data from T2HKK and DUNE. We showed also the *CP* violation sensitivity in these experiments as a function of $\delta_{24}(\text{true})$ when $\delta_{13}(\text{true})$ and $\delta_{34}(\text{true})$ were allowed to take all possible values and the corresponding sensitivity was plotted as a band. Finally, we showed the *CP* violation sensitivity by marginalizing over the hierarchy. It was seen that the *CP* sensitivity of T2HK for $\delta_{13}(\text{true}) = \pi/2$ goes down. However, for T2HKK and T2HKK+DUNE the sensitivity remains mostly unchanged mainly due to the fact that these setups are able to resolve the issue of hierarchy themselves owing to their longer baselines.

We also showed how the expected mass hierarchy sensitivity of T2HK, T2HKK and T2HKK+DUNE changes in the presence of sterile mixing. Here the effect of increasing the value of the sterile mixing angle was shown to have an interesting effect on the corresponding expected sensitivity of the T2HK and T2HKK setups. When the sterile mixing angles are taken to be small, the neutrino mass hierarchy sensitivity of T2HK and T2HKK is seen to deteriorate in the $3+1$ case compared to the $3+0$ case, for some values of $\delta_{13}(\text{true})$, $\delta_{24}(\text{true})$ and $\delta_{34}(\text{true})$. However, when the sterile mixing angles were increased the mass hierarchy sensitivity of T2HK and T2HKK increased for nearly all values of $\delta_{13}(\text{true})$, $\delta_{24}(\text{true})$ and $\delta_{34}(\text{true})$. The reason for this behavior was traced to the effect of marginalization over $|\Delta m^2_{31}|$.

Finally, we presented the expected octant of θ_{23} sensitivity of T2HK, T2HKK and T2HKK+DUNE in the $3+1$ scenario. We showed results for both choices of LO and HO and for two sets of true sterile mixing values and the full range of all three phases $\delta_{13}(\text{true})$, $\delta_{24}(\text{true})$ and $\delta_{34}(\text{true})$. Again for this case, the expected octant sensitivity appears to be mostly decreasing in the $3+1$ case compared to the $3+0$ case when the mixing angles are small. But when the true sterile mixing angles are taken to be larger, the octant sensitivity is seen to improve for some sets of values of $\delta_{13}(\text{true})$, $\delta_{24}(\text{true})$ and $\delta_{34}(\text{true})$, especially for T2HKK and T2HKK combined with DUNE.

ACKNOWLEDGMENTS

We acknowledge the HRI cluster computing facility [51]. The authors would like to thank the Department of Atomic Energy (DAE) Neutrino Project under the XII plan of Harish-Chandra Research Institute. This project has received funding from the European Union's Horizon 2020 research and innovation program InvisiblesPlus RISE under the Marie Sklodowska-Curie Grant Agreement No. 690575. This project has received funding from the European Union's Horizon 2020 research and innovation program Elusives ITN under the Marie Sklodowska-Curie Grant Agreement No. 674896.

[1] R. Acciarri *et al.* (DUNE Collaboration), arXiv:1601.02984.
[2] J. Strait *et al.* (DUNE Collaboration), arXiv:1601.05823.
[3] R. Acciarri *et al.* (DUNE Collaboration), arXiv:1512.06148.
[4] R. Acciarri *et al.* (DUNE Collaboration), arXiv:1601.05471.
[5] K. Abe *et al.* (Hyper-Kamiokande Proto-Collaboration), Prog. Theor. Exp. Phys. **2015**, 53C02 (2015).
[6] K. Abe *et al.* (Hyper-Kamiokande proto-Collaboration), arXiv:1611.06118.
[7] K. N. Abazajian *et al.*, arXiv:1204.5379.
[8] C. Athanassopoulos *et al.* (LSND Collaboration), Phys. Rev. Lett. **75**, 2650 (1995).
[9] A. Aguilar-Arevalo *et al.* (LSND Collaboration), Phys. Rev. D **64**, 112007 (2001).
[10] H. Gemmeke *et al.*, Nucl. Instrum. Methods Phys. Res., Sect. A **289**, 490 (1990).
[11] A. A. Aguilar-Arevalo *et al.* (MiniBooNE Collaboration), Phys. Rev. Lett. **98**, 231801 (2007).
[12] A. A. Aguilar-Arevalo *et al.* (MiniBooNE Collaboration), Phys. Rev. Lett. **110**, 161801 (2013).
[13] A. A. Aguilar-Arevalo *et al.* (MiniBooNE Collaboration), Phys. Rev. Lett. **105**, 181801 (2010).
[14] G. Mention, M. Fechner, T. Lasserre, T. A. Mueller, D. Lhuillier, M. Cribier, and A. Letourneau, Phys. Rev. D **83**, 073006 (2011).
[15] T. A. Mueller *et al.*, Phys. Rev. C **83**, 054615 (2011).
[16] P. Huber, Phys. Rev. C **84**, 024617 (2011); **85**, 029901(E) (2012).
[17] J. N. Abdurashitov *et al.*, Phys. Rev. C **73**, 045805 (2006).
[18] J. N. Bahcall, P. I. Krastev, and E. Lisi, Phys. Lett. B **348**, 121 (1995).
[19] C. Giunti and M. Laveder, Mod. Phys. Lett. A **22**, 2499 (2007).
[20] C. Giunti and M. Laveder, Phys. Rev. D **82**, 053005 (2010).
[21] C. Giunti and M. Laveder, Phys. Rev. C **83**, 065504 (2011).
[22] S. Schael *et al.* (SLD Electroweak Group, DELPHI, ALEPH, SLD, SLD Heavy Flavour Group, OPAL, LEP Electroweak Working Group, and L3 Collaborations), Phys. Rep. **427**, 257 (2006).
[23] S. Goswami, Phys. Rev. D **55**, 2931 (1997).
[24] M. Lattanzi (Planck Collaboration), J. Phys. Conf. Ser. **718**, 032008 (2016).
[25] J. Kopp, P. A. N. Machado, M. Maltoni, and T. Schwetz, J. High Energy Phys. 05 (2013) 050.
[26] N. Klop and A. Palazzo, Phys. Rev. D **91**, 073017 (2015).
[27] R. Gandhi, B. Kayser, M. Masud, and S. Prakash, J. High Energy Phys. 11 (2015) 039.
[28] S. Choubey and D. Pramanik, Phys. Lett. B **764**, 135 (2017).
[29] J. M. Berryman, A. de Gouva, K. J. Kelly, and A. Kobach, Phys. Rev. D **92**, 073012 (2015).
[30] K. J. Kelly, Phys. Rev. D **95**, 115009 (2017).
[31] S. K. Agarwalla, S. S. Chatterjee, A. Dasgupta, and A. Palazzo, J. High Energy Phys. 02 (2016) 111.
[32] M. Ghosh, S. Gupta, Z. M. Matthews, P. Sharma, and A. G. Williams, arXiv:1704.04771.
[33] S. K. Agarwalla, S. S. Chatterjee, and A. Palazzo, J. High Energy Phys. 09 (2016) 016.
[34] S. K. Agarwalla, S. S. Chatterjee, and A. Palazzo, Phys. Rev. Lett. **118**, 031804 (2017).
[35] D. Dutta, R. Gandhi, B. Kayser, M. Masud, and S. Prakash, J. High Energy Phys. 11 (2016) 122.
[36] P. Huber, M. Lindner, and W. Winter, Comput. Phys. Commun. **167**, 195 (2005).
[37] P. Huber, J. Kopp, M. Lindner, M. Rolinec, and W. Winter, Comput. Phys. Commun. **177**, 432 (2007).
[38] J. Kopp, Int. J. Mod. Phys. C **19**, 523 (2008); **19**, 845(E) (2008).
[39] J. Kopp, M. Lindner, T. Ota, and J. Sato, Phys. Rev. D **77**, 013007 (2008).
[40] I. Esteban, M. C. Gonzalez-Garcia, M. Maltoni, I. Martinez-Soler, and T. Schwetz, J. High Energy Phys. 01 (2017) 087.
[41] Y. Declais *et al.*, Nucl. Phys. **B434**, 503 (1995).
[42] F. P. An *et al.* (Daya Bay Collaboration), Phys. Rev. Lett. **113**, 141802 (2014).
[43] P. Adamson *et al.* (MINOS, Daya Bay Collaboration), Phys. Rev. Lett. **117**, 151801 (2016); **117**, 209901 (2016).
[44] Y. Ko *et al.*, Phys. Rev. Lett. **118**, 121802 (2017).
[45] M. G. Aartsen *et al.* (IceCube Collaboration), Phys. Rev. Lett. **117**, 071801 (2016).

[46] P. Adamson *et al.* (MINOS Collaboration), Phys. Rev. Lett. **107**, 011802 (2011).
[47] P. Adamson *et al.* (NOνA Collaboration), arXiv:1706.04592.
[48] K. Bora, D. Dutta, and P. Ghoshal, J. High Energy Phys. 12 (2012) 025.
[49] S. Gariazzo, C. Giunti, M. Laveder, and Y. F. Li, J. High Energy Phys. 06 (2017) 135.
[50] Y. Fukuda *et al.* (Super-Kamiokande Collaboration), Phys. Rev. Lett. **81**, 1562 (1998).
[51] http://cluster.hri.res.in.